Available online at www.sciencedirect.com
ScienceDirect
Journal of Sound and Vibration 314 (2008) 757–774
JOURNAL OF SOUND AND VIBRATION
www.elsevier.com/locate/jsvi

Nonlinear transversal vibration and stability of an axially moving viscoelastic string supported by a partial viscoelastic guide

Mergen H. Ghayesh*

Mechanical Engineering Department, School of Engineering, Tarbiat Modarres University, Tehran, Iran

Received 9 July 2007; received in revised form 31 October 2007; accepted 4 January 2008
Handling Editor: L.G. Tham
Available online 4 March 2008

Abstract

In this paper, transversal nonlinear vibration of an axially moving viscoelastic string supported by a partial viscoelastic guide is analytically investigated. The string is traveling under time-variant velocity, which includes a mean velocity along with small harmonic fluctuations. The model of the viscoelastic guide is also a parallel combination of springs and viscous dampers. The governing partial-differential equation is derived from Hamilton's principle and geometrical relations. The method of multiple scales is applied to the governing partial-differential equation to obtain solvability conditions for both non-resonance and principal parametric resonance cases. Additionally, in the case of principal parametric resonance, the stability and bifurcation of trivial and non-trivial steady-state responses are analyzed through the Routh–Hurwitz criterion. Eventually, numerical simulations are presented to highlight the effects of mean velocity, guide length, stiffness and damping coefficient of the guide and viscosity coefficient of the string on the natural frequencies, stability, frequency-response curves and bifurcation points of the system.

1. Introduction

Axially moving systems can be simple models of many engineering devices, such as paper sheets, power transition chains, fiber textiles, band saw blades, magnetic tapes and conveyor belts.

A significant amount of research has been carried out on axially moving systems in various pieces of literatures. Wickert [1] considered nonlinear vibration of an axially moving beam in sub- and supercritical traveling velocity. Stylianou and Tabarrok [2] obtained numerical solutions of an axially moving beam through the finite element method (FEM). They have also investigated the effects of tip mass and high frequency of axial motion fluctuations on transverse vibrations of the system. Stylianou and Tabarrok [3] used FEM to examine the effects of wall flexibility, damping and tip support on the stability of the system. Furthermore, Oz et al. [4] investigated the transition behavior between a string and a beam using the

*Tel.: +98 021 88011001 3346.
E-mail address: mergenh@gmail.com

0022-460X/$ - see front matter © 2008 Elsevier Ltd. All rights reserved.
doi:10.1016/j.jsv.2008.01.030

perturbation method. Pakdemirli et al. [5] investigated the transverse vibration of an axially moving string through the Galerkin method and by discretizing the equations. Pakdemirli and Ozkay [6] used the method of multiple scales and obtained a boundary layer solution for an axially moving beam under constant speed. Pellicano and Zirilli [7] analyzed the oscillation of an axially moving beam under an assumption of weak nonlinearities. Parker [8] examined the stability of an axially moving string supported by a discrete elastic guide. Chakraborty et al. [9] studied free and forced responses of a nonlinear traveling slender beam. Oz and Pakdemirli [10] investigated the vibrations of an axially moving beam under time-variant velocity. They used the multiple-scales methods to investigate principal parametric resonances in detail. Oz et al. [11] investigated the nonlinear vibration and stability of an axially moving beam with time-variant velocity. They used the multiple-scales method to obtain solvability conditions for three cases. Chen et al. [12] obtained a bifurcation diagram versus dynamic viscosity, transport speed and periodic perturbation for a string. Shin et al. [13] investigated the vibrations of a membrane using the Galerkin method to discretize the equations of motion and investigate the effects of system parameters on the natural frequencies, mode shapes and stability of a system. Zhang and Chen [14] investigated the nonlinear behavior of an axially moving viscoelastic string. Chen and Zhao [15] investigated the transverse vibration of an axially moving beam under a low axial speed. Chen et al. [16] solved the transverse vibration equations of an axially moving string through the modified finite difference method. Chen and Yang [17] considered an axially moving viscoelastic beam under time-variant velocity. Kartik and Wickert [18] investigated the forced vibration of an axially moving strip, which is guided by a partial elastic foundation and edge imperfection. Chen and Yang [19] considered two models of nonlinear vibration of an axially moving beam, and then they compared the results of the two models. Marynowski and Kapitaniak [20] considered an axially moving beam as a three-parameter Zener element. They then used the Galerkin method to discretize the equations of motion. Ha et al. [21] investigated chaos and bifurcation of a three-dimensional moving viscoelastic string. Ghayesh [22] compared nonlinear vibration and stability conditions of two dynamic models of axially moving Timoshenko beams. Ghayesh and Khadem [23] investigated rotary inertia and temperature effects on nonlinear vibration of an axially moving beam.

From all the above-mentioned researches, it can be concluded that the vast majority of researches were devoted to the beam model of axially moving materials [1–4,6,7,9–11,15,17,19,20,22,23], and the others considered the string model [5,8,12,14,16,18,21]. Axially moving materials can also be modeled as a plate, shell and membrane [13].

In the classical models of axially moving systems, the traveling speed is assumed to be constant with respect to time [1,7,8], whereas some other recent researches state that the speed is assumed to be time variant [10,11,17,19,22,23]. In such cases, the speed is comprised of a mean velocity along with small harmonic fluctuations.

Axially moving materials can also be modeled as linear [4,8,10,18] or nonlinear [1,7,9,11] systems. Although the nonlinear systems are difficult to deal with analytically, they can explain the model behavior with more precision than linear ones.

Since, considering that the energy-dissipative mechanisms in axially moving materials make models more close to reality, viscoelascity, as an effective approach to model the energy-dissipative mechanisms, was considered in Refs. [14,17].

In the following, the transversal nonlinear vibration and stability of an axially moving viscoelastic string supported by a partial viscoelastic guide are investigated analytically. After deriving the governing partial-differential equation of motion, the multiple-scales method is applied and stability conditions are obtained through the Ruth–Hurwitz criterion. Finally, the numerical simulations are presented to show the effects of system parameters on the natural frequencies, stability and bifurcation points of the system.

2. Equations of motion

A viscoelastic string, which is supported by a viscoelastic guide is depicted in Fig. 1. This string, with an axial stiffness of EA, is under applied pretension of T and a time-variant transport speed of $v(t^*)$.

To derive the equations of motion through the energy method, three segments of the string will be considered. The first segment is the span where $0<x^*<a$, the second is the span where $a<x^*<(a+b)$ and the third is the span where $(a+b)<x^*<(a+b+c)$.

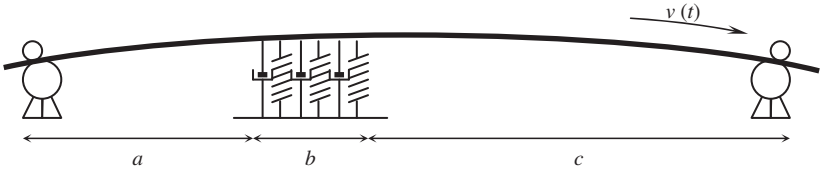

Fig. 1. An axially moving viscoelastic string on a partial viscoelastic guide.

The equations of motion will further be obtained for each segment in the upcoming sections.

Considering only transversal displacement, the kinetic energy in the span $0<x^*<a$, is given by

$$T_a = \frac{1}{2}\rho A \int_0^a \left(\frac{\partial u^*}{\partial t^*} + v\frac{\partial u^*}{\partial x^*}\right)^2 \mathrm{d}x^* \tag{1}$$

in which x^* and $u^*(x^*, t^*)$ are the spatial variable and transversal displacement of the string, respectively. Also, the nonlinear disturbed strain of an infinitesimal element of the string, as well as the potential energy of the whole system, are found by

$$\varepsilon_{x^*} = \frac{1}{2}\left(\frac{\partial u^*}{\partial x^*}\right)^2, \tag{2}$$

$$U_a = \int_0^a \left(\frac{1}{2}T\left(\frac{\partial u^*}{\partial x^*}\right)^2 + \frac{1}{8}\mathrm{EA}\left(\frac{\partial u^*}{\partial x^*}\right)^4\right)\mathrm{d}x^*. \tag{3}$$

In the Kelvin–Voigt model for viscoelastic materials, the constitution relation is

$$\sigma = E\varepsilon_{x^*} + \hat{\eta}\frac{\partial \varepsilon_{x^*}}{\partial t^*}, \tag{4}$$

where σ, ε_{x^*} and $\hat{\eta}$ are the distributed stress, distributed strain and viscosity coefficient of the string, respectively.

The variation of work of the non-conservative force due to the viscosity of the string can be written as [12,14,17]

$$\begin{aligned}(\delta w_{\mathrm{nc}})_a^{\mathrm{visco}} &= \int_0^a \frac{\partial}{\partial x^*}\left(\hat{\eta}\frac{\partial \varepsilon_{x^*}}{\partial t^*}\frac{\partial u^*}{\partial x^*}\right)\delta u^*\,\mathrm{d}x^* \\ &= \int_0^a \hat{\eta}A\left[\frac{\partial^3 u^*}{\partial x^{*2}\partial t^*}\left(\frac{\partial u^*}{\partial x^*}\right)^2 + 2\frac{\partial^2 u^*}{\partial x^{*2}}\frac{\partial u^*}{\partial x^*}\frac{\partial^2 u^*}{\partial x^*\partial t^*}\right]\delta u^*\,\mathrm{d}x^*.\end{aligned} \tag{5}$$

Then the governing equation of the span $0<x^*<a$ can be derived through Hamilton's principal:

$$\int_{t_1^*}^{t_2^*}\left[\delta T_a - \delta U_a + (\delta w_{\mathrm{nc}})_a^{\mathrm{visco}}\right]\mathrm{d}t^* = 0. \tag{6}$$

Substitution of Eqs. (1), (2) and (5) into Eq. (6) will lead to

$$\begin{aligned}&\rho A\left[\frac{\partial^2 u^*}{\partial t^{*2}} + \frac{\partial v}{\partial t^*}\frac{\partial u^*}{\partial x^*} + 2v\frac{\partial^2 u^*}{\partial x^*\partial t^*} + \left(v^2 - \frac{T}{\rho A}\right)\frac{\partial^2 u^*}{\partial x^{*2}}\right] \\ &\quad = \frac{3}{2}\mathrm{EA}\left(\frac{\partial u^*}{\partial x^*}\right)^2\frac{\partial^2 u^*}{\partial x^{*2}} + \hat{\eta}A\left[\frac{\partial^3 u^*}{\partial x^{*2}\partial t^*}\left(\frac{\partial u^*}{\partial x^*}\right)^2 + 2\frac{\partial^2 u^*}{\partial x^{*2}}\frac{\partial u^*}{\partial x^*}\frac{\partial^2 u^*}{\partial x^*\partial t^*}\right].\end{aligned} \tag{7}$$

Introducing dimensionless quantities

$$\begin{aligned}\hat{u} &= u^*/(a+b+c),\\ x &= x^*/(a+b+c),\\ t &= t^*\sqrt{T/\rho A(a+b+c)^2},\\ c_v(t) &= v\sqrt{\rho A/T}\end{aligned} \tag{8}$$

and simplifying Eq. (7), one has

$$\frac{\partial^2\hat{u}}{\partial t^2}+\frac{\partial c_v}{\partial t}\frac{\partial\hat{u}}{\partial x}+2c_v\frac{\partial^2\hat{u}}{\partial x\partial t}+(c_v^2-1)\frac{\partial^2\hat{u}}{\partial x^2}=\frac{3}{2}\mu^2\left(\frac{\partial\hat{u}}{\partial x}\right)^2\frac{\partial^2\hat{u}}{\partial x^2}+\eta\left[\frac{\partial^3\hat{u}}{\partial x^2\partial t}\left(\frac{\partial\hat{u}}{\partial x}\right)^2+2\frac{\partial^2\hat{u}}{\partial x^2}\frac{\partial\hat{u}}{\partial x}\frac{\partial^2\hat{u}}{\partial x\partial t}\right] \tag{9}$$

in which

$$\begin{aligned}\mu &= \sqrt{\mathrm{EA}/T},\\ \eta &= \sqrt{\hat{\eta}^2A/T\rho(a+b+c)^2}.\end{aligned} \tag{10}$$

Using transformation $\hat{u}=\sqrt{\varepsilon}u^{(a)}$ ($\varepsilon\ll1$) and substituting it into Eq. (9) one has

$$\begin{aligned}&\frac{\partial^2u^{(a)}}{\partial t^2}+\frac{\partial c_v}{\partial t}\frac{\partial u^{(a)}}{\partial x}+2c_v\frac{\partial^2u^{(a)}}{\partial x\partial t}+(c_v^2-1)\frac{\partial^2u^{(a)}}{\partial x^2}\\ &\quad=\frac{3}{2}\mu^2\varepsilon\left(\frac{\partial u^{(a)}}{\partial x}\right)^2\frac{\partial^2u^{(a)}}{\partial x^2}+\eta\varepsilon\left[\frac{\partial^3u^{(a)}}{\partial x^2\partial t}\left(\frac{\partial u^{(a)}}{\partial x}\right)^2+2\frac{\partial^2u^{(a)}}{\partial x^2}\frac{\partial u^{(a)}}{\partial x}\frac{\partial^2u^{(a)}}{\partial x\partial t}\right].\end{aligned} \tag{11}$$

Eq. (11) is the governing equation of motion of the span $0<x^*<a$ or $(0<x<a/(a+b+c))$. The governing equation of the span $(a+b)<x^*<(a+b+c)$ or $(a+b/(a+b+c)<x<1)$ can be derived using a similar procedure of Eqs. (1)–(11). Then the equation of motion of the span $(a+b)<x^*<(a+b+c)$ is of the form

$$\begin{aligned}&\frac{\partial^2u^{(c)}}{\partial t^2}+\frac{\partial c_v}{\partial t}\frac{\partial u^{(c)}}{\partial x}+2c_v\frac{\partial^2u^{(c)}}{\partial x\partial t}+(c_v^2-1)\frac{\partial^2u^{(c)}}{\partial x^2}\\ &\quad=\frac{3}{2}\mu^2\varepsilon\left(\frac{\partial u^{(c)}}{\partial x}\right)^2\frac{\partial^2u^{(c)}}{\partial x^2}+\eta\varepsilon\left[\frac{\partial^3u^{(c)}}{\partial x^2\partial t}\left(\frac{\partial u^{(c)}}{\partial x}\right)^2+2\frac{\partial^2u^{(c)}}{\partial x^2}\frac{\partial u^{(c)}}{\partial x}\frac{\partial^2u^{(c)}}{\partial x\partial t}\right].\end{aligned} \tag{12}$$

For the span $a<x^*<(a+b)$, which is subjected to the viscoelastic guide, i.e. a parallel combination of the springs and viscous dampers, the kinetic and potential energy will be in the form

$$T_b=\frac{1}{2}\rho A\int_a^{a+b}\left(\frac{\partial u^*}{\partial t^*}+v\frac{\partial u^*}{\partial x^*}\right)^2\mathrm{d}x^*, \tag{13}$$

$$U_b=\int_a^{a+b}\left(\frac{1}{2}T\left(\frac{\partial u^*}{\partial x^*}\right)^2+\frac{1}{8}\mathrm{EA}\left(\frac{\partial u^*}{\partial x^*}\right)^4\right)\mathrm{d}x^*+\frac{1}{2}\int_a^{a+b}ku^{*^2}\,\mathrm{d}x^* \tag{14}$$

in which k is the stiffness coefficient per unit length of the guide.

The variation of the work of the non-conservative force due to the viscosity of the guide can be illustrated as

$$(\delta w_{\mathrm{nc}})^g=-\int_a^{a+b}\hat{\zeta}\left(\frac{\partial u^*}{\partial t^*}+v\frac{\partial u^*}{\partial x^*}\right)\delta u^*\,\mathrm{d}x^*, \tag{15}$$

where $\hat{\zeta}$ is the damping coefficient per unit length of the guide.

The variation of the work due to the viscosity of the string can be illustrated by the form of Eq. (5), i.e.

$$(\delta w_{\mathrm{nc}})_b^{\mathrm{visco}}=\int_a^{a+b}\frac{\partial}{\partial x^*}\left(\hat{\eta}\frac{\partial\varepsilon_{x^*}}{\partial t^*}\frac{\partial u^*}{\partial x^*}\right)\delta u^*\,\mathrm{d}x^*=\int_a^{a+b}\hat{\eta}A\left[\frac{\partial^3u^*}{\partial x^{*^2}\partial t^*}\left(\frac{\partial u^*}{\partial x^*}\right)^2+2\frac{\partial^2u^*}{\partial x^{*^2}}\frac{\partial u^*}{\partial x^*}\frac{\partial^2u^*}{\partial x^*\partial t^*}\right]\delta u^*\,\mathrm{d}x^*. \tag{16}$$

Then using Eqs. (13)–(16), Hamilton's principle will lead to

$$\int_{t_1^*}^{t_2^*}(\delta T_b-\delta U_b+(\delta w_{\rm nc})^g+(\delta w_{\rm nc})_b^{\rm visco})\,{\rm d}t^*=0, \tag{17}$$

$$\begin{aligned}&\rho A\left[\frac{\partial^2 u^*}{\partial t^{*^2}}+\frac{\partial v}{\partial t^*}\frac{\partial u^*}{\partial x^*}+2v\frac{\partial^2 u^*}{\partial x^*\partial t^*}+\left(v^2-\frac{T}{\rho A}\right)\frac{\partial^2 u^*}{\partial x^{*^2}}\right]+ku^*+\hat{\zeta}\left(\frac{\partial u^*}{\partial t^*}+v\frac{\partial u^*}{\partial x^*}\right)\\&=\frac{3}{2}{\rm EA}\left(\frac{\partial u^*}{\partial x^*}\right)^2\frac{\partial^2 u^*}{\partial x^{*^2}}+\hat{\eta}A\left[\frac{\partial^3 u^*}{\partial x^{*^2}\partial t^*}\left(\frac{\partial u^*}{\partial x^*}\right)^2+2\frac{\partial^2 u^*}{\partial x^{*^2}}\frac{\partial u^*}{\partial x^*}\frac{\partial^2 u^*}{\partial x^*\partial t^*}\right].\end{aligned} \tag{18}$$

Using dimensionless quantities of Eqs. (8), Eq. (18) can be rewritten as

$$\begin{aligned}&\frac{\partial^2\hat{u}}{\partial t^2}+\frac{\partial c_v}{\partial t}\frac{\partial\hat{u}}{\partial x}+2c_v\frac{\partial^2\hat{u}}{\partial x\partial t}+(c_v^2-1)\frac{\partial^2\hat{u}}{\partial x^2}+\kappa^2\hat{u}+\zeta\left(\frac{\partial\hat{u}}{\partial t}+c_v\frac{\partial\hat{u}}{\partial x}\right)\\&=\frac{3}{2}\mu^2\left(\frac{\partial\hat{u}}{\partial x}\right)^2\frac{\partial^2\hat{u}}{\partial x^2}+\eta\left[\frac{\partial^3\hat{u}}{\partial x^2\partial t}\left(\frac{\partial\hat{u}}{\partial x}\right)^2+2\frac{\partial^2\hat{u}}{\partial x^2}\frac{\partial\hat{u}}{\partial x}\frac{\partial^2\hat{u}}{\partial x\partial t}\right]\end{aligned} \tag{19}$$

in which

$$\begin{aligned}\kappa&=\sqrt{k(a+b+c)^2/T},\\\zeta&=\sqrt{\hat{\zeta}^2(a+b+c)^2/\rho AT}.\end{aligned} \tag{20}$$

Transformation of $\hat{u}=\sqrt{\varepsilon}u^{(b)}$ ($\varepsilon\ll 1$) makes Eq. (19) in the form

$$\begin{aligned}&\frac{\partial^2 u^{(b)}}{\partial t^2}+\frac{\partial c_v}{\partial t}\frac{\partial u^{(b)}}{\partial x}+2c_v\frac{\partial^2 u^{(b)}}{\partial x\partial t}+(c_v^2-1)\frac{\partial^2 u^{(b)}}{\partial x^2}+\kappa^2u^{(b)}+\zeta\left(\frac{\partial u^{(b)}}{\partial t}+c_v\frac{\partial u^{(b)}}{\partial x}\right)\\&=\frac{3}{2}\mu^2\varepsilon\left(\frac{\partial u^{(b)}}{\partial x}\right)^2\frac{\partial^2 u^{(b)}}{\partial x^2}+\eta\varepsilon\left[\frac{\partial^3 u^{(b)}}{\partial x^2\partial t}\left(\frac{\partial u^{(b)}}{\partial x}\right)^2+2\frac{\partial^2 u^{(b)}}{\partial x^2}\frac{\partial u^{(b)}}{\partial x}\frac{\partial^2 u^{(b)}}{\partial x\partial t}\right].\end{aligned} \tag{21}$$

As mentioned above, the string is moving with a time-variant velocity, which is comprised of a harmonic velocity about a constant mean velocity, i.e.

$$c_v(t)=\overline{c}+\varepsilon c_0\,\sin(\alpha t) \tag{22}$$

in which α is the frequency of varying speed, $\overline{c}$ is the mean velocity and εc_0 is amplitude of the speed.

Substitution of Eq. (22) into Eq. (11), for the span $0<x^*<a$, into Eq. (21) for the span $a<x^*<a+b$, and into Eq. (12), for the span $a+b<x^*<a+b+c$, respectively, will lead to

$$\begin{aligned}&\frac{\partial^2 u^{(a)}}{\partial t^2}+(\varepsilon c_0\alpha\,\cos(\alpha t))\frac{\partial u^{(a)}}{\partial x}+2(\overline{c}+\varepsilon c_0\,\sin(\alpha t))\frac{\partial^2 u^{(a)}}{\partial x\partial t}+(\overline{c}^2-1+\varepsilon^2c_0^2\sin^2(\alpha t)+2\varepsilon\overline{c}c_0\,\sin(\alpha t))\frac{\partial^2 u^{(a)}}{\partial x^2}\\&=\frac{3}{2}\mu^2\varepsilon\left(\frac{\partial u^{(a)}}{\partial x}\right)^2\frac{\partial^2 u^{(a)}}{\partial x^2}+\eta\varepsilon\left[\frac{\partial^3 u^{(a)}}{\partial x^2\partial t}\left(\frac{\partial u^{(a)}}{\partial x}\right)^2+2\frac{\partial^2 u^{(a)}}{\partial x^2}\frac{\partial u^{(a)}}{\partial x}\frac{\partial^2 u^{(a)}}{\partial x\partial t}\right],\end{aligned} \tag{23}$$

$$\begin{aligned}&\frac{\partial^2 u^{(b)}}{\partial t^2}+(\varepsilon c_0\alpha\,\cos(\alpha t))\frac{\partial u^{(b)}}{\partial x}+2(\overline{c}+\varepsilon c_0\,\sin(\alpha t))\frac{\partial^2 u^{(b)}}{\partial x\partial t}+(\overline{c}^2-1+\varepsilon^2c_0^2\sin^2(\alpha t)\\&\quad+2\varepsilon\overline{c}c_0\,\sin(\alpha t))\frac{\partial^2 u^{(b)}}{\partial x^2}+\kappa^2u^{(b)}+\zeta\left(\frac{\partial u^{(b)}}{\partial t}+(\overline{c}+\varepsilon c_0\,\sin(\alpha t))\frac{\partial u^{(b)}}{\partial x}\right)\\&=\frac{3}{2}\mu^2\varepsilon\left(\frac{\partial u^{(b)}}{\partial x}\right)^2\frac{\partial^2 u^{(b)}}{\partial x^2}+\eta\varepsilon\left[\frac{\partial^3 u^{(b)}}{\partial x^2\partial t}\left(\frac{\partial u^{(b)}}{\partial x}\right)^2+2\frac{\partial^2 u^{(b)}}{\partial x^2}\frac{\partial u^{(b)}}{\partial x}\frac{\partial^2 u^{(b)}}{\partial x\partial t}\right],\end{aligned} \tag{24}$$

$$\frac{\partial^2 u^{(c)}}{\partial t^2}+(\varepsilon c_0\alpha\,\cos(\alpha t))\frac{\partial u^{(c)}}{\partial x}+2(\overline{c}+\varepsilon c_0\,\sin(\alpha t))\frac{\partial^2 u^{(c)}}{\partial x\partial t}+(\overline{c}^2-1+\varepsilon^2 c_0^2\sin^2(\alpha t)+2\varepsilon\overline{c}c_0\,\sin(\alpha t))\frac{\partial^2 u^{(c)}}{\partial x^2}$$
$$=\frac{3}{2}\mu^2\varepsilon\left(\frac{\partial u^{(c)}}{\partial x}\right)^2\frac{\partial^2 u^{(c)}}{\partial x^2}+\eta\varepsilon\left[\frac{\partial^3 u^{(c)}}{\partial x^2\partial t}\left(\frac{\partial u^{(c)}}{\partial x}\right)^2+2\frac{\partial^2 u^{(c)}}{\partial x^2}\frac{\partial u^{(c)}}{\partial x}\frac{\partial^2 u^{(c)}}{\partial x\partial t}\right]. \tag{25}$$

3. Direct multiple-scales method

The straightforward expansion techniques fail to correctly represent a proper solution for problems, which have secular terms. This deficiency is overcome by permitting the solution to be a function of multiple independent time variables, or scales [24].

In the method of multiple scales, one assumes the expansion in the form [25–27]

$$u^{(j)}(x,t;\varepsilon)=u_0^{(j)}(x,T_0,T_1)+\varepsilon u_1^{(j)}(x,T_0,T_1)+\cdots,\quad j=a,b,c \tag{26}$$

in which $T_0=t$ and $T_1=\varepsilon t$.

Substitution of Eq. (26) into Eqs. (23) and (25) yields

$$O(\varepsilon^0):\quad D_0^2u_0^{(j)}+2\overline{c}D_0\left(\frac{\partial u_0^{(j)}}{\partial x}\right)+(\overline{c}^2-1)\frac{\partial^2 u_0^{(j)}}{\partial x^2}=0,\quad j=a,c, \tag{27}$$

$$O(\varepsilon^1):\quad D_0^2u_1^{(j)}+2\overline{c}D_0\left(\frac{\partial u_1^{(j)}}{\partial x}\right)+(\overline{c}^2-1)\frac{\partial^2 u_1^{(j)}}{\partial x^2}=-2D_0D_1u_0^{(j)}-c_0\alpha\,\cos(\alpha t)$$
$$\times\frac{\partial u_0^{(j)}}{\partial x}-2c_0\,\sin(\alpha t)D_0\left(\frac{\partial u_0^{(j)}}{\partial x}\right)-2\overline{c}D_1\left(\frac{\partial u_0^{(j)}}{\partial x}\right)-2\overline{c}c_0\,\sin(\alpha t)\frac{\partial^2 u_0^{(j)}}{\partial x^2}$$
$$+\frac{3}{2}\mu^2\left(\frac{\partial u_0^{(j)}}{\partial x}\right)^2\frac{\partial^2 u_0^{(j)}}{\partial x^2}+\eta\left[D_0\left(\frac{\partial^2 u_0^{(j)}}{\partial x^2}\right)\left(\frac{\partial u_0^{(j)}}{\partial x}\right)^2+2\frac{\partial^2 u_0^{(j)}}{\partial x^2}\frac{\partial u_0^{(j)}}{\partial x}D_0\left(\frac{\partial u_0^{(j)}}{\partial x}\right)\right],\quad j=a,c, \tag{28}$$

where $D_0=\mathrm{d}/\mathrm{d}T_0$ and $D_1=\mathrm{d}/\mathrm{d}T_1$.

For the span $a<x^*<a+b$, which is supported by the distributed viscoelastic guide, Eqs. (24) and (26) will lead to

$$O(\varepsilon^0):\quad D_0^2u_0^{(b)}+2\overline{c}D_0\left(\frac{\partial u_0^{(b)}}{\partial x}\right)+(\overline{c}^2-1)\frac{\partial^2 u_0^{(b)}}{\partial x^2}+\kappa^2u_0^{(b)}+\zeta\left(D_0u_0^{(b)}+\overline{c}\frac{\partial u_0^{(b)}}{\partial x}\right)=0, \tag{29}$$

$$O(\varepsilon^1):\quad D_0^2u_1^{(b)}+2\overline{c}D_0\left(\frac{\partial u_1^{(b)}}{\partial x}\right)+(\overline{c}^2-1)\frac{\partial^2 u_1^{(b)}}{\partial x^2}+\kappa^2u_1^{(b)}+\zeta\left(D_0u_1^{(b)}+\overline{c}\frac{\partial u_1^{(b)}}{\partial x}\right)$$
$$=-2D_0D_1u_0^{(b)}-c_0\alpha\,\cos(\alpha t)\times\frac{\partial u_0^{(b)}}{\partial x}-2c_0\,\sin(\alpha t)\times D_0\left(\frac{\partial u_0^{(b)}}{\partial x}\right)$$
$$-2\overline{c}D_1\left(\frac{\partial u_0^{(b)}}{\partial x}\right)-2\overline{c}c_0\,\sin(\alpha t)\times\frac{\partial^2 u_0^{(b)}}{\partial x^2}$$
$$-\zeta D_1u_0^{(b)}-\zeta c_0\,\sin(\alpha t)\times\frac{\partial u_0^{(b)}}{\partial x}+\frac{3}{2}\mu^2\left(\frac{\partial u_0^{(b)}}{\partial x}\right)^2\frac{\partial^2 u_0^{(b)}}{\partial x^2}$$
$$+\eta\left[D_0\left(\frac{\partial^2 u_0^{(b)}}{\partial x^2}\right)\left(\frac{\partial u_0^{(b)}}{\partial x}\right)^2+2\frac{\partial^2 u_0^{(b)}}{\partial x^2}\frac{\partial u_0^{(b)}}{\partial x}D_0\left(\frac{\partial u_0^{(b)}}{\partial x}\right)\right]. \tag{30}$$

4. Mode shapes of the system

One supposes that the solution of Eq. (27) is in the form [10,11,17,19,22,23]

$$u_0^{(j)}(x,T_0,T_1)=\sum_{n=1}^{\infty}[A_n(T_1)\mathrm{e}^{\mathrm{i}\omega_n T_0}u_n^{(j)}(x)+\overline{A}_n(T_1)\mathrm{e}^{-\mathrm{i}\omega_n T_0}\,\overline{u}_n^{(j)}(x)],\quad j=a,b,c, \tag{31}$$

where A_n is the nth amplitude, $u_n^{(j)}(x)$ the nth complex mode shape and ω_n the nth natural frequency.

To obtain the nth complex mode shape, $u_n^{(j)}(x)$, for the span which is not subjected to the viscoelastic guide, substituting Eq. (31) into Eq. (27), one has

$$(1-\overline{c}^2)\frac{\mathrm{d}^2u_n^{(j)}}{\mathrm{d}x^2}-2\mathrm{i}\overline{c}\omega_n\frac{\mathrm{d}u_n^{(j)}}{\mathrm{d}x}+\omega_n^2u_n^{(j)}=0,\quad j=a,c. \tag{32}$$

Assuming the solution of Eq. (32) of the exponential form

$$u_n^{(j)}(x)=\mathrm{e}^{\mathrm{i}\mu_n x},\quad j=a,c. \tag{33}$$

Eq. (32) will lead to

$$\mu_{1n}=\frac{-\omega_n}{\overline{c}+1},\quad \mu_{2n}=\frac{\omega_n}{1-\overline{c}}. \tag{34}$$

Then using Eqs. (33) and (34), the nth complex mode shape for the spans $0<x^*<a$ and $a+b<x^*<a+b+c$ will be obtained as

$$u_n^{(j)}(x)=c_{1n}^{(j)}\mathrm{e}^{\mathrm{i}\mu_{1n}x}+c_{2n}^{(j)}\mathrm{e}^{\mathrm{i}\mu_{2n}x},\quad j=a,c \tag{35}$$

in which $c_{1n}^{(j)}$ and $c_{2n}^{(j)}$ are constants.

For the span where $a<x^*<a+b$, which is subjected to the viscoelastic guide, substitution of Eq. (31) into Eq. (29) leads to

$$(1-\overline{c}^2)\frac{\mathrm{d}^2u_n^{(b)}}{\mathrm{d}x^2}-(2\mathrm{i}\omega_n+\zeta)\overline{c}\frac{\mathrm{d}u_n^{(b)}}{\mathrm{d}x}+(\omega_n^2-\zeta\mathrm{i}\omega_n-\kappa^2)u_n^{(b)}=0. \tag{36}$$

One assumes that the mode shape, $u_n^{(b)}$, is of the form $u_n^{(b)}(x)=\exp(\mathrm{i}\varphi_n x)$; then Eq. (36) leads to

$$\varphi_{1n,2n}=\frac{\mathrm{i}\zeta\overline{c}-2\overline{c}\omega_n\pm\sqrt{4\kappa^2(\overline{c}^2-1)+4\omega_n^2-4\mathrm{i}\omega_n\zeta-\zeta^2\overline{c}^2}}{2(\overline{c}^2-1)}. \tag{37}$$

Through Eq. (37), the nth complex mode shape for the span $a<x^*<a+b$ becomes

$$u_n^{(b)}(x)=c_{1n}^{(b)}\mathrm{e}^{\mathrm{i}\varphi_{1n}x}+c_{2n}^{(b)}\mathrm{e}^{\mathrm{i}\varphi_{2n}x} \tag{38}$$

in which $c_{1n}^{(b)}$ and $c_{2n}^{(b)}$ are constants.

Replacing the mean velocity by minus one in Eq. (37), will lead to $\overline{u}_{nn}^{(b)}$, which will be used in the following sections. To determine the constants of the above equations, the boundary and compatibility conditions of the system at $x^*=a,a+b,a+b+c$ must be satisfied, i.e.

$$c_{1n}^{(a)}+c_{2n}^{(a)}=0, \tag{39}$$

$$c_{1n}^{(c)}\mathrm{e}^{\mathrm{i}\mu_{1n}(a+b+c)}+c_{2n}^{(c)}\mathrm{e}^{\mathrm{i}\mu_{2n}(a+b+c)}=0, \tag{40}$$

$$c_{1n}^{(a)}\mathrm{e}^{\mathrm{i}\mu_{1n}a}+c_{2n}^{(a)}\mathrm{e}^{\mathrm{i}\mu_{2n}a}=c_{1n}^{(b)}\mathrm{e}^{\mathrm{i}\varphi_{1n}a}+c_{2n}^{(b)}\mathrm{e}^{\mathrm{i}\varphi_{2n}a}, \tag{41}$$

$$c_{1n}^{(b)}\mathrm{e}^{\mathrm{i}\varphi_{1n}(a+b)}+c_{2n}^{(b)}\mathrm{e}^{\mathrm{i}\varphi_{2n}(a+b)}=c_{1n}^{(c)}\mathrm{e}^{\mathrm{i}\mu_{1n}(a+b)}+c_{2n}^{(c)}\mathrm{e}^{\mathrm{i}\mu_{2n}(a+b)}, \tag{42}$$

$$c_{1n}^{(a)}\mathrm{i}\mu_{1n}\mathrm{e}^{\mathrm{i}\mu_{1n}a}+c_{2n}^{(a)}\mathrm{i}\mu_{2n}\mathrm{e}^{\mathrm{i}\mu_{2n}a}=c_{1n}^{(b)}\mathrm{i}\varphi_{1n}\mathrm{e}^{\mathrm{i}\varphi_{1n}a}+c_{2n}^{(b)}\mathrm{i}\varphi_{2n}\mathrm{e}^{\mathrm{i}\varphi_{2n}a}, \tag{43}$$

$$c_{1n}^{(b)}\mathrm{i}\varphi_{1n}\mathrm{e}^{\mathrm{i}\varphi_{1n}(a+b)}+c_{2n}^{(b)}\mathrm{i}\varphi_{2n}\mathrm{e}^{\mathrm{i}\varphi_{2n}(a+b)}=c_{1n}^{(c)}\mathrm{i}\mu_{1n}\mathrm{e}^{\mathrm{i}\mu_{1n}(a+b)}+c_{2n}^{(c)}\mathrm{i}\mu_{2n}\mathrm{e}^{\mathrm{i}\mu_{2n}(a+b)}. \tag{44}$$

Assuming $c_{2n}^{(c)}$ is equal to unity, other coefficients can be obtained through the process of elimination in Eqs. (39)–(44); then one has

$$c_{1n}^{(b)} = \left(\frac{\mu_{1n}-\varphi_{2n}}{\varphi_{2n}-\varphi_{1n}}\right)\exp\left[\mathrm{i}\left((\mu_{2n}-\mu_{1n})(a+b+c)+(\mu_{1n}-\varphi_{1n})(a+b)\right)\right] + \left(\frac{\varphi_{2n}-\mu_{2n}}{\varphi_{2n}-\varphi_{1n}}\right)\exp\left[\mathrm{i}\left((\mu_{2n}-\varphi_{1n})(a+b)\right)\right], \tag{45}$$

$$c_{2n}^{(b)} = \left(\frac{\varphi_{1n}-\mu_{1n}}{\varphi_{2n}-\varphi_{1n}}\right)\exp\left[\mathrm{i}\left((\mu_{2n}-\mu_{1n})(a+b+c)+(\mu_{1n}-\varphi_{2n})(a+b)\right)\right] + \left(\frac{\mu_{2n}-\varphi_{1n}}{\varphi_{2n}-\varphi_{1n}}\right)\exp\left[\mathrm{i}\left((\mu_{2n}-\varphi_{2n})(a+b)\right)\right], \tag{46}$$

$$\begin{aligned} c_{1n}^{(a)} = {} & \left(\frac{\mu_{2n}-\varphi_{1n}}{\mu_{2n}-\mu_{1n}}\right)\left(\frac{\mu_{1n}-\varphi_{2n}}{\varphi_{2n}-\varphi_{1n}}\right)\exp\left[\mathrm{i}((\varphi_{1n}-\mu_{1n})a+(\mu_{2n}-\mu_{1n})(a+b+c)+(\mu_{1n}-\varphi_{1n})(a+b))\right] \\ & + \left(\frac{\mu_{2n}-\varphi_{1n}}{\mu_{2n}-\mu_{1n}}\right)\left(\frac{\varphi_{2n}-\mu_{2n}}{\varphi_{2n}-\varphi_{1n}}\right)\exp\left[\mathrm{i}((\varphi_{1n}-\mu_{1n})a+(\mu_{2n}-\varphi_{1n})(a+b))\right] \\ & + \left(\frac{\mu_{2n}-\varphi_{2n}}{\mu_{2n}-\mu_{1n}}\right)\left(\frac{\varphi_{1n}-\mu_{1n}}{\varphi_{2n}-\varphi_{1n}}\right)\exp\left[\mathrm{i}((\varphi_{2n}-\mu_{1n})a+(\mu_{2n}-\mu_{1n})(a+b+c)+(\mu_{1n}-\varphi_{2n})(a+b))\right] \\ & + \left(\frac{\mu_{2n}-\varphi_{2n}}{\mu_{2n}-\mu_{1n}}\right)\left(\frac{\mu_{2n}-\varphi_{1n}}{\varphi_{2n}-\varphi_{1n}}\right)\exp\left[\mathrm{i}((\varphi_{2n}-\mu_{1n})a+(\mu_{2n}-\varphi_{2n})(a+b))\right], \end{aligned} \tag{47}$$

$$\begin{aligned} c_{2n}^{(a)} = {} & \left(\frac{\varphi_{1n}-\mu_{1n}}{\mu_{2n}-\mu_{1n}}\right)\left(\frac{\mu_{1n}-\varphi_{2n}}{\varphi_{2n}-\varphi_{1n}}\right)\exp[\mathrm{i}((\varphi_{1n}-\mu_{2n})a+(\mu_{2n}-\mu_{1n})(a+b+c)+(\mu_{1n}-\varphi_{1n})(a+b))] \\ & + \left(\frac{\varphi_{1n}-\mu_{1n}}{\mu_{2n}-\mu_{1n}}\right)\left(\frac{\varphi_{2n}-\mu_{2n}}{\varphi_{2n}-\varphi_{1n}}\right)\exp[\mathrm{i}((\varphi_{1n}-\mu_{2n})a+(\mu_{2n}-\varphi_{1n})(a+b))] \\ & + \left(\frac{\varphi_{2n}-\mu_{1n}}{\mu_{2n}-\mu_{1n}}\right)\left(\frac{\varphi_{1n}-\mu_{1n}}{\varphi_{2n}-\varphi_{1n}}\right)\exp[\mathrm{i}((\varphi_{2n}-\mu_{2n})a+(\mu_{2n}-\mu_{1n})(a+b+c)+(\mu_{1n}-\varphi_{2n})(a+b))] \\ & + \left(\frac{\varphi_{2n}-\mu_{1n}}{\mu_{2n}-\mu_{1n}}\right)\left(\frac{\mu_{2n}-\varphi_{1n}}{\varphi_{2n}-\varphi_{1n}}\right)\exp[\mathrm{i}((\varphi_{2n}-\mu_{2n})a+(\mu_{2n}-\varphi_{2n})(a+b))], \end{aligned} \tag{48}$$

$$c_{1n}^{(c)} = -\mathrm{e}^{\mathrm{i}(\mu_{2n}-\mu_{1n})(a+b+c)}. \tag{49}$$

Substituting Eqs. (45)–(49) into Eqs. (35) and (38), mode shapes of the system can be easily obtained.

5. Solvability conditions

This section is devoted to obtain solvability conditions for the non-resonance and principal parametric resonance cases.

To investigate the solvability conditions, the generality of $u_0^{(a)}$, $u_0^{(b)}$ and $u_0^{(c)}$ will not be lost if only the nth mode of vibration is considered [10,11,17,19,22,23]:

$$u_0^{(j)}(x,T_0,T_1) = A_n(T_1)\mathrm{e}^{\mathrm{i}\omega_n T_0}u_n^{(j)}(x) + \overline{A}_n(T_1)\mathrm{e}^{-\mathrm{i}\omega_n T_0}\overline{u}_n^{(j)}(x), \quad j=a,b,c. \tag{50}$$

Substitution of Eq. (50) into Eqs. (28) and (30) will lead to

$$\begin{aligned} O(\varepsilon^1): \ & D_0^2u_1^{(j)} + 2\overline{c}D_0\left(\frac{\partial u_1^{(j)}}{\partial x}\right) + (\overline{c}^2-1)\frac{\partial^2 u_1^{(j)}}{\partial x^2} \\ & = \left[3\mu^2A_n^2\overline{A}_n\left(\frac{1}{2}\left(u_n'^{(j)}\right)^2\overline{u}_n''^{(j)} + u_n''^{(j)}u_n'^{(j)}\overline{u}_n'^{(j)}\right) - 2\dot{A}_n\left(\mathrm{i}\omega_n u_n^{(j)} + \overline{c}u_n'^{(j)}\right)\right]\exp(\mathrm{i}\omega_n T_0) \end{aligned}$$

$$+\left[-\frac{1}{2}c_0\alpha u_n'^{(j)}-c_0\omega_n u_n'^{(j)}+\mathrm{i}\bar{c}c_0u_n''^{(j)}\right]A_n\exp(\mathrm{i}(\alpha+\omega_n)T_0)+\left[-\frac{1}{2}c_0\alpha\overline{u}_n'^{(j)}+c_0\omega_n\overline{u}_n'^{(j)}+\mathrm{i}\bar{c}c_0u_n''^{(j)}\right]$$
$$\times\overline{A}_n\exp(\mathrm{i}(\alpha-\omega_n)T_0)+\eta A_n^2\overline{A}_n\mathrm{i}\omega_n\left[2u_n''^{(j)}u_n'^{(j)}\overline{u}_n'^{(j)}+\overline{u}_n''^{(j)}\left(u_n'^{(j)}\right)^2\right]\exp(\mathrm{i}\omega_nT_0)+cc+\mathrm{NST},\quad j=a,c, \tag{51}$$

$$O(\varepsilon^1):\quad D_0^2u_1^{(b)}+2\bar{c}D_0\left(\frac{\partial u_1^{(b)}}{\partial x}\right)+(\bar{c}^2-1)\frac{\partial^2u_1^{(b)}}{\partial x^2}+\kappa^2u_1^{(b)}+\zeta\left(D_0u_1^{(b)}+\bar{c}\frac{\partial u_1^{(b)}}{\partial x}\right)$$
$$=\left[3\mu^2A_n^2\overline{A}_n\left(\frac{1}{2}\left(u_n'^{(b)}\right)^2\overline{u}_n''^{(j)}+u_n''^{(b)}u_n'^{(b)}\overline{u}_n'^{(b)}\right)-2\dot{A}_n\left(\mathrm{i}\omega_nu_n^{(b)}+\bar{c}u_n'^{(b)}\right)-\zeta\dot{A}_nu_n^{(b)}\right]\exp(\mathrm{i}\omega_nT_0)$$
$$+\left[-\frac{1}{2}c_0\alpha u_n'^{(b)}-c_0\omega_nu_n'^{(b)}+\mathrm{i}\bar{c}c_0u_n''^{(b)}+\frac{1}{2}\zeta\mathrm{i}c_0u_n'^{(b)}\right]A_n\exp(\mathrm{i}(\alpha+\omega_n)T_0)$$
$$+\left[-\frac{1}{2}c_0\alpha\overline{u}_n'^{(b)}+c_0\omega_n\overline{u}_n'^{(b)}+\mathrm{i}\bar{c}c_0\overline{u}_n''^{(b)}+\frac{1}{2}\zeta\mathrm{i}c_0\overline{u}_n'^{(b)}\right]\overline{A}_n\exp(\mathrm{i}(\alpha-\omega_n)T_0)$$
$$+\eta A_n^2\overline{A}_n\mathrm{i}\omega_n\left[2u_n''^{(b)}u_n'^{(b)}\overline{u}_n'^{(b)}+\overline{u}_n''^{(b)}\left(u_n'^{(b)}\right)^2\right]\exp(\mathrm{i}\omega_nT_0)+cc+\mathrm{NST} \tag{52}$$

in which the prime and the dot denote, respectively, derivation with respect to spatial variable x and slow time variable T_1.

The solvability condition demands that every solution of the homogeneous part of Eqs. (51) and (52) must be orthogonal to its right-hand side [27]. Then, from Eqs. (51) and (52), the solvability condition for the non-resonance case will be

$$\dot{A}_n(2\alpha_2+\zeta\alpha_4)-A_n^2\overline{A}_n(3\mu^2\alpha_1+\eta\mathrm{i}\omega_n\alpha_3)=0 \tag{53}$$

in which

$$\alpha_1=\frac{1}{2}\left\{\int_0^{a/(a+b+c)}\left[\left(u_n'^{(a)}\right)^2u_n''^{(a)}\overline{u}_n^{(a)}+2u_n''^{(a)}u_n'^{(a)}\overline{u}_n'^{(a)}\overline{u}_n^{(a)}\right]\mathrm{d}x\right.$$
$$+\int_{(a+b)/(a+b+c)}^1\left[\left(u_n'^{(c)}\right)^2\overline{u}_n''^{(c)}\overline{u}_n^{(c)}+2u_n''^{(c)}u_n'^{(c)}\overline{u}_n'^{(c)}\overline{u}_n^{(c)}\right]\mathrm{d}x$$
$$\left.+\int_{a/(a+b+c)}^{(a+b)/(a+b+c)}\left[\left(u_n'^{(b)}\right)^2\overline{u}_n''^{(b)}\overline{u}_{nn}^{(b)}+2u_n''^{(b)}u_n'^{(b)}\overline{u}_n'^{(b)}\overline{u}_{nn}^{(b)}\right]\mathrm{d}x\right\}, \tag{54}$$

$$\alpha_2=\int_0^{a/(a+b+c)}\left[\mathrm{i}\omega_nu_n^{(a)}\overline{u}_n^{(a)}+\bar{c}u_n'^{(a)}\overline{u}_n^{(a)}\right]\mathrm{d}x+\int_{(a+b)/(a+b+c)}^1\left[\mathrm{i}\omega_nu_n^{(c)}\overline{u}_n^{(c)}+\bar{c}u_n'^{(c)}\overline{u}_n^{(c)}\right]\mathrm{d}x$$
$$+\int_{a/(a+b+c)}^{(a+b)/(a+b+c)}\left[\mathrm{i}\omega_nu_n^{(b)}\overline{u}_{nn}^{(b)}+\bar{c}u_n'^{(b)}\overline{u}_{nn}^{(b)}\right]\mathrm{d}x, \tag{55}$$

$$\alpha_3=\int_0^{a/(a+b+c)}\left[2u_n''^{(a)}u_n'^{(a)}\overline{u}_n'^{(a)}\overline{u}_n^{(a)}+u_n''^{(a)}\left(u_n'^{(a)}\right)^2\overline{u}_n^{(a)}\right]\mathrm{d}x$$
$$+\int_{(a+b)/(a+b+c)}^1\left[2u_n''^{(c)}u_n'^{(c)}\overline{u}_n'^{(c)}\overline{u}_n^{(c)}+u_n''^{(c)}\left(u_n'^{(c)}\right)^2\overline{u}_n^{(c)}\right]\mathrm{d}x$$
$$+\int_{a/(a+b+c)}^{(a+b)/(a+b+c)}\left[2u_n''^{(b)}u_n'^{(b)}\overline{u}_n'^{(b)}\overline{u}_{nn}^{(b)}+u_n''^{(b)}\left(u_n'^{(b)}\right)^2\overline{u}_{nn}^{(b)}\right]\mathrm{d}x, \tag{56}$$

$$\alpha_4 = \int_{a/(a+b+c)}^{(a+b)/(a+b+c)} u_n^{(b)} \overline{u}_{nn}^{(b)} \, \mathrm{d}x. \tag{57}$$

In the case of principal parametric resonance, using Eqs. (51) and (52) and assuming $\alpha = 2\omega_n + \varepsilon\sigma$ in which σ is the detuning parameter, one has

$$\dot{A}_n(2\alpha_2 + \zeta\alpha_4) - A_n^2\overline{A}_n(3\mu^2\alpha_1 + \eta \mathrm{i}\omega_n\alpha_3) - c_0\alpha_5\overline{A}_n \exp(\mathrm{i}\sigma T_1) = 0, \tag{58}$$

where

$$\begin{aligned}\alpha_5 = {} & \left(\omega_n - \frac{1}{2}\alpha\right)\left\{\int_0^{a/(a+b+c)} \overline{u}_n'^{(a)}\overline{u}_n^{(a)} \, \mathrm{d}x + \int_{a/(a+b+c)}^{(a+b)/(a+b+c)} \overline{u}_n'^{(b)}\overline{u}_{nn}^{(b)} \, \mathrm{d}x + \int_{(a+b)/(a+b+c)}^{1} \overline{u}_n'^{(c)}\overline{u}_n^{(c)} \, \mathrm{d}x\right\} \\ & + \mathrm{i}\bar{c}\left\{\int_0^{a/(a+b+c)} \overline{u}_n''^{(a)}\overline{u}_n^{(a)} \, \mathrm{d}x + \int_{a/(a+b+c)}^{(a+b)/(a+b+c)} \overline{u}_n''^{(b)}\overline{u}_{nn}^{(b)} \, \mathrm{d}x + \int_{(a+b)/(a+b+c)}^{1} \overline{u}_n''^{(a)}\overline{u}_n^{(c)} \, \mathrm{d}x\right\} \\ & + \frac{1}{2}\zeta\mathrm{i}\int_{a/(a+b+c)}^{(a+b)/(a+b+c)} \overline{u}_n'^{(b)}\overline{u}_{nn}^{(b)} \, \mathrm{d}x.\end{aligned} \tag{59}$$

6. Stability

In this section, stability conditions of the principal parametric resonance case will be discussed. After constructing the Jacobian matrix and evaluating the eigenvalues, the Routh–Hurwitz criterion will be used to obtain the local stability conditions.

To cover the goals mentioned above, Eq. (58) can be rewritten in the form of the following equation:

$$\dot{A}_n - A_n^2\overline{A}_n(\mu^2\mu_\alpha + \eta\eta_\alpha) - c_0c_\alpha\overline{A}_n \exp(\mathrm{i}\sigma T_1) = 0, \tag{60}$$

where

$$\mu_\alpha = \frac{3\alpha_1}{(2\alpha_2 + \zeta\alpha_4)}, \tag{61}$$

$$\eta_\alpha = \frac{\mathrm{i}\omega_n\alpha_3}{(2\alpha_2 + \zeta\alpha_4)}, \tag{62}$$

$$c_\alpha = \frac{\alpha_5}{(2\alpha_2 + \zeta\alpha_4)}. \tag{63}$$

Assuming A_n of the polar form

$$A_n(T_1) = \tfrac{1}{2}a_n(T_1)\mathrm{e}^{\mathrm{i}\beta_n(T_1)} \tag{64}$$

and substituting it into Eq. (60) will lead to the modulation equations

$$a_n' = \tfrac{1}{4}a_n^3(\mu^2\mu_{\alpha r} + \eta\eta_{\alpha r}) + c_0a_n(c_{\alpha r}\cos\gamma_n - c_{\alpha i}\sin\gamma_n), \tag{65}$$

$$\gamma_n'a_n = \sigma a_n - \tfrac{1}{2}a_n^3(\mu^2\mu_{\alpha i} + \eta\eta_{\alpha i}) - 2c_0a_n(c_{\alpha r}\sin\gamma_n + c_{\alpha i}\cos\gamma_n), \tag{66}$$

where

$$\left\{\begin{array}{c}\mu_\alpha = \mu_{\alpha r} + \mathrm{i}\mu_{\alpha i} \\ \eta_\alpha = \eta_{\alpha r} + \mathrm{i}\eta_{\alpha i} \\ c_\alpha = c_{\alpha r} + \mathrm{i}c_{\alpha i} \\ \gamma_n = \sigma T_1 - 2\beta_n\end{array}\right\}. \tag{67}$$

Stationary responses of the system will be one of its equilibrium points, and so when all derivatives with respect to the slow time variable is equal to zero, Eqs. (65) and (66) result in the first detuning parameter,

σ_1, and the second detuning parameter, σ_2,

$$\sigma_{1,2} = \frac{1}{2}a_n^2(\mu^2\mu_{\alpha i} + \eta\eta_{\alpha i}) \mp 2\sqrt{c_0^2(c_{\alpha r}^2 + c_{\alpha i}^2) - \left[\frac{1}{4}a_n^2(\mu^2\mu_{\alpha r} + \eta\eta_{\alpha r})\right]^2}. \tag{68}$$

The Jacobian matrix of the system can also be constructed as

$$\tilde{J} = \begin{bmatrix} \frac{3}{4}a_n^2(\mu^2\mu_{\alpha r} + \eta\eta_{\alpha r}) + c_0(c_{\alpha r}\cos\gamma_n - c_{\alpha i}\sin\gamma_n) & -c_0a_n(c_{\alpha r}\sin\gamma_n + c_{\alpha i}\cos\gamma_n) \\ -a_n(\mu^2\mu_{\alpha i} + \eta\eta_{\alpha i}) & -2c_0(c_{\alpha r}\cos\gamma_n - c_{\alpha i}\sin\gamma_n) \end{bmatrix}. \tag{69}$$

Using the modulation equations, evaluating eigenvalues of the Jacobian matrix results in

$$\begin{aligned} &\lambda^2 - a_n^2(\mu^2\mu_{\alpha r} + \eta\eta_{\alpha r})\lambda + \tfrac{1}{4}a_n^4(\mu^2\mu_{\alpha r} + \eta\eta_{\alpha r})^2 + \tfrac{1}{4}a_n^4(\mu^2\mu_{\alpha i} + \eta\eta_{\alpha i})^2 \\ &\quad - \tfrac{1}{2}a_n^2\sigma(\mu^2\mu_{\alpha i} + \eta\eta_{\alpha i}) = 0. \end{aligned} \tag{70}$$

Then for the first and the second detuning parameters, σ_1 and σ_2, the eigenvalue equations become

$$\begin{aligned} &\lambda^2 - a_n^2(\mu^2\mu_{\alpha r} + \eta\eta_{\alpha r})\lambda + \frac{1}{4}a_n^4(\mu^2\mu_{\alpha r} + \eta\eta_{\alpha r})^2 \\ &\quad + a_n^2(\mu^2\mu_{\alpha i} + \eta\eta_{\alpha i})\sqrt{c_0^2(c_{\alpha r}^2 + c_{\alpha i}^2) - \left[\frac{1}{4}a_n^2(\mu^2\mu_{\alpha r} + \eta\eta_{\alpha r})\right]^2} = 0, \end{aligned} \tag{71}$$

$$\begin{aligned} &\lambda^2 - a_n^2(\mu^2\mu_{\alpha r} + \eta\eta_{\alpha r})\lambda + \frac{1}{4}a_n^4(\mu^2\mu_{\alpha r} + \eta\eta_{\alpha r})^2 \\ &\quad - a_n^2(\mu^2\mu_{\alpha i} + \eta\eta_{\alpha i})\sqrt{c_0^2(c_{\alpha r}^2 + c_{\alpha i}^2) - \left[\frac{1}{4}a_n^2(\mu^2\mu_{\alpha r} + \eta\eta_{\alpha r})\right]^2} = 0. \end{aligned} \tag{72}$$

From Eqs. (71) and (72), through the Routh–Hurwitz criterion, the stability conditions for the first and the second detuning parameters, respectively, become

$$\left\{ \begin{array}{c} -\dfrac{4c_0|c_\alpha|}{a_n^2} < \mu^2\mu_{\alpha r} + \eta\eta_{\alpha r} < \dfrac{4c_0|c_\alpha|}{a_n^2} \\ (\mu^2\mu_{\alpha r} + \eta\eta_{\alpha r}) < 0 \\ (\mu^2\mu_{\alpha i} + \eta\eta_{\alpha i}) > 0 \end{array} \right\}, \tag{73}$$

$$\left\{ \begin{array}{c} -\dfrac{4c_0|c_\alpha|}{a_n^2} < \mu^2\mu_{\alpha r} + \eta\eta_{\alpha r} < \dfrac{4c_0|c_\alpha|}{a_n^2} \\ (\mu^2\mu_{\alpha r} + \eta\eta_{\alpha r}) < 0 \\ (\mu^2\mu_{\alpha i} + \eta\eta_{\alpha i}) < 0 \end{array} \right\}. \tag{74}$$

7. Numerical simulations

In this section, the numerical simulations are presented to show the effectiveness of analytic solutions. The objectives of this section are to investigate the mean velocity, stiffness and damping coefficients of the guide, guide length, nonlinearity and the viscosity coefficients of the string on the natural frequencies, stability, frequency-response curves and bifurcation points of the system.

Using Eqs. (39)–(44) and applying the solvability conditions for non-trivial solutions of $c_{1n}^{(j)}$ and $c_{2n}^{(j)}$, $j = a, b, c$ one can obtain the natural frequencies of the system.

In Table 1, the first natural frequency of the system is depicted in terms of the guide stiffness and the mean velocity variations for the case, in which $\zeta = 4.32$, $a = 0.2$, $b = 0.7$, $c = 0.1$. Table 1 shows that the increasing mean velocity will decrease the first natural frequency while the increasing stiffness factor of the guide

increases the first natural frequency of the system. Table 2 shows the effects of the guide stiffness and mean velocity on the second natural frequency of the system. As can be concluded from Table 3, the natural frequencies of the system decrease when the guide length decreases. In Tables 4 and 5, the effects of damping coefficient of the guide on the first and the second natural frequencies of the system are shown. Tables 4 and 5 demonstrate that increasing not only the mean velocity but also the damping coefficient factor of the guide will lead to a reduction in the first and the second natural frequencies of the system.

Frequency-response curves of the system in the principal parametric resonance case are shown in Fig. 2 for the various stiffness factors of the guide (κ). There are two bifurcation points in the system: the first bifurcation point is located at $\sigma = \sigma_1$, in which a stable non-trivial solution bifurcates from the trivial solution, and the second one is located at $\sigma = \sigma_2$, where an unstable non-trivial solution bifurcates from an unstable trivial solution. In Fig. 2, the curves which correspond to $\kappa = 1$, 2.3, 3.1, the slope of curves and instability areas of trivial solutions are, respectively, 1/59.65, 1/34.61, 1/20.27 and 4.98, 3.9, 2.9. Therefore, numerical simulations show that the increasing stiffness factor of the guide makes the first bifurcation point

Table 1
The first natural frequency, ω_1, versus the mean velocity and stiffness factor of the guide ($\zeta = 4.32$, $a = 0.2$, $b = 0.7$, $c = 0.1$)

$\overline{c}$	$\kappa = 3.26$	$\kappa = 4.38$	$\kappa = 4.9$	$\kappa = 6.3$
0.00	3.995896	4.903906	5.351239	6.593561
0.04	3.975585	4.893549	5.340749	6.582296
0.08	3.954800	4.872178	5.318837	6.558345
0.12	3.923669	4.839797	5.285503	6.521711
0.16	3.882199	4.796401	5.240737	6.472381
0.20	3.830396	4.741976	5.184515	6.410334
0.24	3.768264	4.676499	5.116804	6.335543
0.28	3.695805	4.599938	5.037559	6.247987
0.32	3.613020	4.512256	4.946731	6.147668
0.36	3.519911	4.413411	4.844265	6.034638
0.40	3.416481	4.303359	4.730112	5.909053
0.44	3.302743	4.182065	4.604242	5.771274
0.48	3.178719	4.049512	4.466668	5.622075
0.52	3.044452	3.905732	4.317498	5.463109
0.56	2.900030	3.750850	4.157019	5.298154
0.60	2.745608	3.585177	4.143289	5.137255

Table 2
The second natural frequency, ω_2, versus the mean velocity and stiffness factor of the guide ($\zeta = 4.32$, $a = 0.2$, $b = 0.7$, $c = 0.1$)

$\overline{c}$	$\kappa = 3.26$	$\kappa = 4.38$	$\kappa = 4.9$	$\kappa = 6.3$
0.00	6.768561	7.272739	7.537504	8.312787
0.04	6.750871	7.254746	7.519262	8.293423
0.08	6.713211	7.216663	7.480811	8.253204
0.12	6.655587	7.158484	7.422133	8.192055
0.16	6.578005	7.080202	7.343208	8.109882
0.20	6.480477	6.981811	7.244014	8.006563
0.24	6.363014	6.863303	7.124522	7.881935
0.28	6.225637	6.724668	6.984695	7.735779
0.32	6.068367	6.565897	6.824485	7.567793
0.36	5.891233	6.386972	6.643828	7.377553
0.40	5.694275	6.187870	6.442633	7.164433
0.44	5.477539	5.968559	6.220770	6.927484
0.48	5.241089	5.728984	5.978045	6.665170
0.52	4.985009	5.469063	5.714159	6.374822
0.56	4.709412	5.188656	5.428627	6.051239
0.60	4.414457	4.887533	5.120621	5.682246

Table 3
The first and the second natural frequencies, ω_1 and ω_2, versus the a ($\zeta = 3.5$, $\kappa = 3.26$, $\bar{c} = 0.2$, $b = 0.6$)

a	ω_1	ω_2
0.00	4.067299430	6.239204336
0.04	4.065443427	6.235469899
0.08	4.056664201	6.222854966
0.12	4.036614811	6.203965510
0.16	4.002692449	6.185640109
0.20	3.954979439	6.171814256
0.24	3.895616021	6.159362007
0.28	3.827000720	6.142122461
0.32	3.750414007	6.118589673
0.36	3.665841315	6.094450115
0.40	3.572713654	6.077373174
0.44	3.470970105	6.070659388
0.48	3.361797643	6.070955508
0.52	3.247601645	6.070097507
0.56	3.131357135	6.059162252
0.60	3.015928948	6.031857895

Table 4
The first natural frequency, ω_1, versus the mean velocity and damping coefficient of the guide ($\kappa = 3.9$, $a = 0.2$, $b = 0.6$, $c = 0.2$)

$\bar{c}$	$\zeta = 0$	$\zeta = 3.5$	$\zeta = 5$	$\zeta = 8$
0.00	3.998336830	3.692713939	3.32888994	1.662013030
0.04	3.993156458	3.687573575	3.32373484	1.655101895
0.08	3.977612972	3.672150891	3.30826800	1.634289688
0.12	3.951699153	3.646441049	3.28248470	1.599329785
0.16	3.915402658	3.610435836	3.24637702	1.549774293
0.20	3.868705506	3.564123422	3.19993370	1.484907131
0.24	3.811583322	3.507488016	3.14313999	1.403620323
0.28	3.744004255	3.440509425	3.07597757	1.304180887
0.32	3.665927483	3.363162494	2.99842441	1.183759554
0.36	3.577301159	3.275416478	2.91045490	1.037358055
0.40	3.478059598	3.177234361	2.81204029	0.854850405
0.44	3.368119365	3.068572291	2.70314979	0.609347447
0.48	3.247373807	2.949379402	2.58375299	0.606347407
0.52	3.115685220	2.819598688	2.45382467	0.580634747
0.56	2.972873430	2.679170354	2.31335413	0.560301680
0.60	2.818698690	2.528040753	2.16236299	0.540809810

appear later and the second one appear sooner. Also, the bend of curves will decrease when the stiffness factor increases.

The frequency-response curves of the system are shown in Fig. 3 for several values of the viscosity coefficient of the string. It can be concluded from Fig. 3 that the locations of bifurcation points are not affected by the viscosity coefficient of the string. In Fig. 3, the curves, which correspond to $\eta = 0$, 0.5, 0.9 and 1.06, have slopes of 1/60.9, 1/57.89, 1/56.12 and 1/55.41. Then the increasing viscosity coefficient of the string will lead to smaller slopes in curves.

In Fig. 4, the effects of the guide length on frequency-response curves are depicted. The slopes of curves and the instability area of trivial solution for systems corresponding to $b = 0$, 0.1, 0.3 are 1/153.32, 25*em*1/138.89, 1/101.18 and 6.00, 4.918, 2.66, respectively. Hence, as shown, both the slopes of curves and the stability area of the trivial solution will increase when the guide length increases. In addition, since the guide length does not affect the stability conditions of the system, then the curve corresponding to the first detuning parameter is stable and the second one is unstable.

Table 5
The second natural frequency, ω_2, versus the mean velocity and damping coefficient of the guide ($\kappa = 3.9$, $a = 0.2$, $b = 0.6$, $c = 0.2$)

$\overline{c}$	$\zeta = 0$	$\zeta = 3.5$	$\zeta = 5$	$\zeta = 8$
0.00	6.644114921	6.587626857	6.51963420	6.241738070
0.04	6.634038940	6.577661562	6.50973709	6.231798411
0.08	6.603810580	6.547767132	6.48004751	6.201976534
0.12	6.553428557	6.497947961	6.43057068	6.152263463
0.16	6.482890672	6.428211544	6.36131536	6.082643361
0.20	6.392193695	6.338568724	6.27229380	5.993092122
0.24	6.281333212	6.229034065	6.16352180	5.883575281
0.28	6.150303384	6.099626330	6.03501846	5.754045046
0.32	5.999096622	5.950369096	5.88680588	5.604436280
0.36	5.827703120	5.781291467	5.71890838	5.434661122
0.40	5.636110212	5.592428866	5.53135092	5.244601900
0.44	5.424301431	5.383823723	5.32415639	5.034101778
0.48	5.192255170	5.155525798	5.09734081	4.802952244
0.52	4.939942678	4.907591342	4.85090533	4.550875595
0.56	4.667325012	4.640079522	4.58482350	4.277497965
0.60	4.374348263	4.353042527	4.29902289	4.102149995

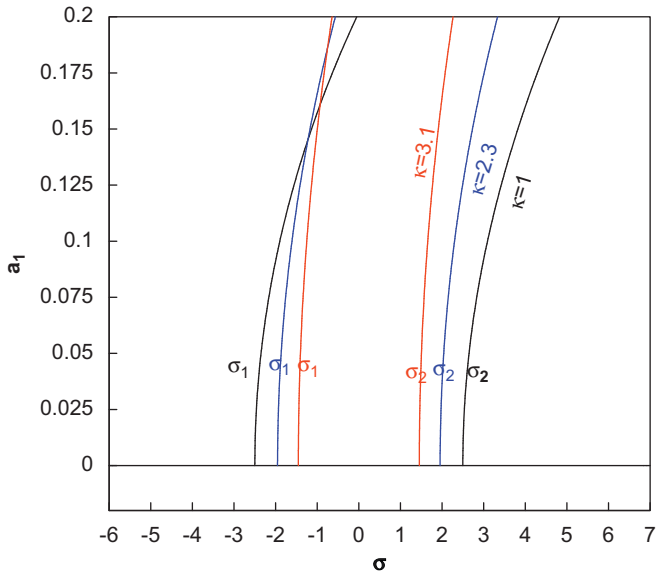

Fig. 2. Frequency-response curve, stability and bifurcation point variations under the guide stiffness factor, κ, variations ($\overline{c} = 0.5$, $\zeta = 2.25$, $a = 0.2$, $b = 0.6$, $c = 0.2$, $\eta = 0.1$, $\mu = 2$), (σ_1: stable, σ_2: unstable).

In Fig. 5, when the nonlinearity coefficient is equal to zero, the system is linear. Increasing the nonlinear coefficient does not affect the instability area of trivial solutions, i.e. the locations of bifurcation points are independent of the nonlinearity terms, while the slope of curves will be increased by increasing nonlinearity term of the system.

The effects of speed fluctuation's amplitude on the frequency-response curves of the system are depicted in Fig. 6. With the increasing speed fluctuation's amplitude, the first bifurcation point will occur earlier, while the second will arise later. The stability of curves, which corresponds to the first and the second detuning parameters, will not be affected by the variations of the speed fluctuation's amplitude.

Fig. 7 shows the effects of the damping coefficient of the guide on the frequency-response curve of the system. The increasing damping coefficient will change the locations of bifurcation points slightly; in other

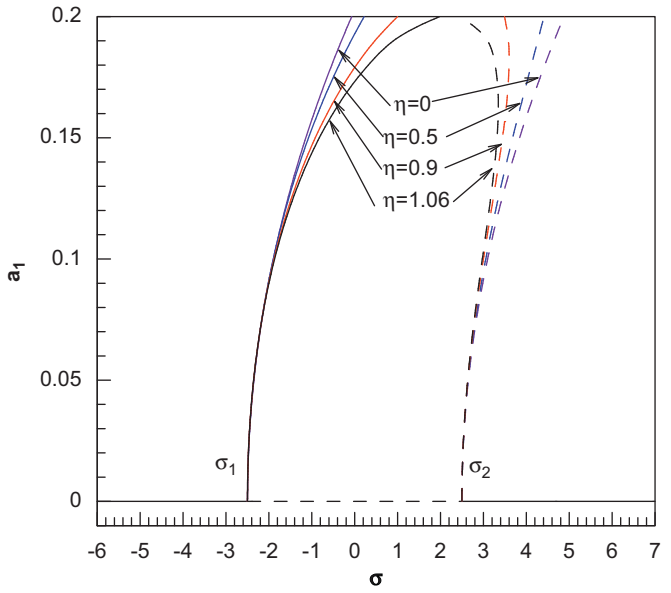

Fig. 3. Frequency-response curve, stability and bifurcation point variations under the string viscosity coefficient, η, variations ($\bar{c} = 0.5$, $\zeta = 2.25$, $\kappa = 1$, $a = 0.2$, $b = 0.6$, $c = 0.2$, $\mu = 2$) (solid line: stable, dashed-line: unstable).

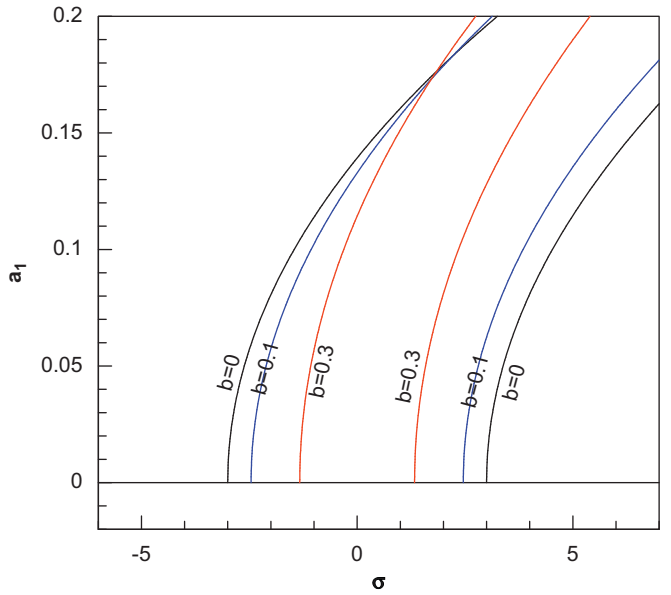

Fig. 4. Frequency-response curve, stability and bifurcation point variations under the guide length, b, variations ($\bar{c} = 0.5$, $\zeta = 2.25$, $\kappa = 1$, $a = 0.2$, $\mu = 2$, $\eta = 0.1$).

words, the instability area of the trivial solution will be increased, but the slopes of the curves will be decreased by the increasing damping coefficient.

8. Summary and conclusions

In this paper, transversal nonlinear vibration and stability of a viscoelastic string supported by a partial viscoelastic guide were investigated. The equations of motion were derived using Hamilton's principle,

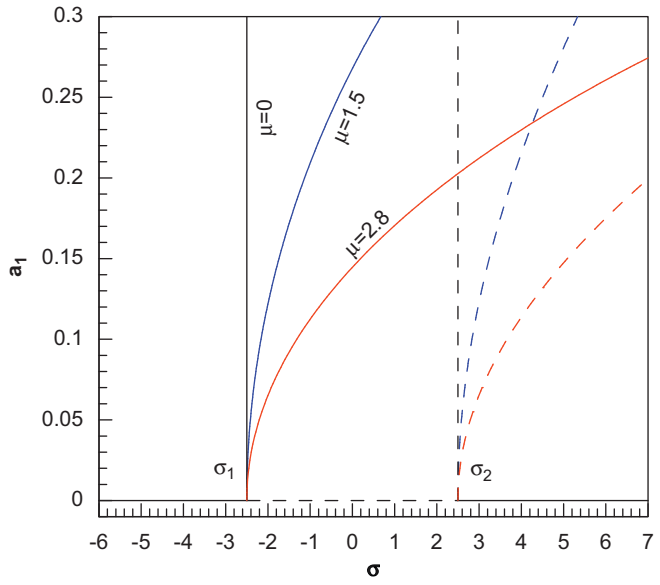

Fig. 5. Frequency-response curve, stability and bifurcation point variations under the nonlinearity coefficient, μ, variations ($\bar{c} = 0.5$, $\zeta = 2.25$, $\kappa = 1$, $a = 0.2$, $b = 0.6$, $c = 0.2$, $\eta = 0.1$) (solid line: stable, dashed-line: unstable).

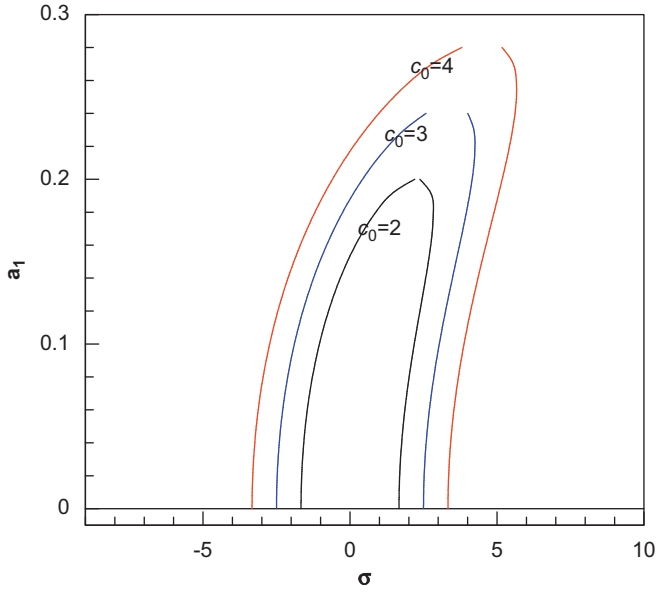

Fig. 6. Frequency-response curve, stability and bifurcation point variations under the speed fluctuation's amplitude, c_0, variations ($\bar{c} = 0.5$, $\zeta = 2.25$, $a = 0.2$, $b = 0.6$, $c = 0.2$, $\eta = 0.65$, $\mu = 2$).

and solvability conditions were analyzed using the multiple-scales method. The stability conditions were obtained through the Routh–Hurwitz criterion for the principal parametric resonance case. Eventually, numerical simulations were carried out to show the effects of the system parameters on the natural frequencies, stability, frequency-response curves and bifurcation points of the system. The more the mean velocity the system experiences, the less the natural frequencies will arise, while the increasing stiffness factor of the guide increases the natural frequencies of the system. The increasing stiffness factor of the guide also makes the first bifurcation point appear later and the second one appear sooner. In addition, the bend of

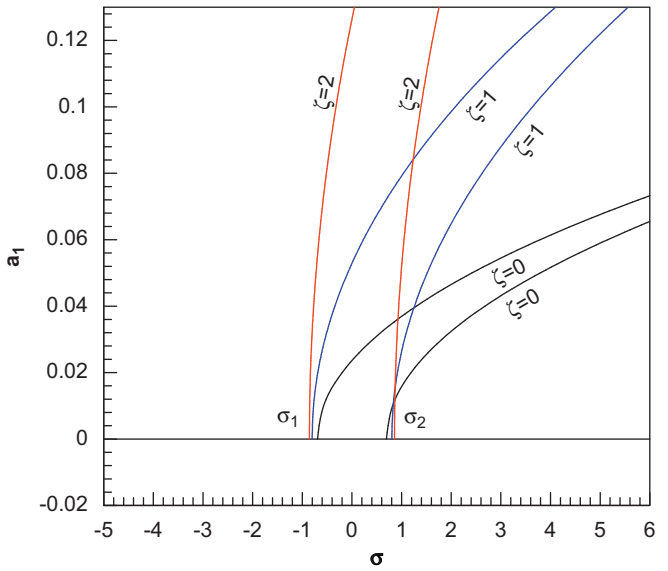

Fig. 7. Frequency-response curve, stability and bifurcation point variations under the damping coefficient of the guide, ζ, variations ($\bar{c} = 0.5$, $\kappa = 3.26$, $a = 0$, $b = 1$, $c = 0$, $\eta = 0.1$, $\mu = 4$) (σ_1: stable, σ_2: unstable).

curves will decrease when the stiffness factor increases. The natural frequencies of the system decrease when the guide length decreases. Both the slopes of curves and the stability area of the trivial solution will increase when the guide length increases. Also, the guide length will not affect the stability conditions of the system; then the curve corresponding to the first detuning parameter remains stable and the second one is unstable.

The increasing damping coefficient of the guide will lead to a reduction in the natural frequencies of the system. It also changes the locations of bifurcation points slightly; in other words, the instability area of the trivial solution will be increased, but the slopes of the curves will be decreased by the increasing damping coefficient. With increasing speed fluctuation's amplitude, the first bifurcation point will occur earlier, while the second will arise later. The stability of curves corresponding to the first and the second detuning parameters will not be affected by the variations of the speed fluctuation's amplitude. The viscosity coefficient variations of the string do not affect the locations of bifurcation points, while increasing the viscosity coefficient of the string will lead to smaller slopes in curves. The locations of bifurcation points are independent of nonlinearity terms, while the slope of curves will be increased by the increasing nonlinearity term of the system.

References

[1] J.A. Wickert, Non-linear vibration of a traveling tensioned beam, *International Journal of Non-linear Mechanics* 27 (1992) 503–517.
[2] M. Stylianou, B. Tabarrok, Finite element analysis of an axially moving beam—part I: time integration, *Journal of Sound and Vibration* 178 (1994) 433–453.
[3] M. Stylianou, B. Tabarrok, Finite element analysis of an axially moving beam—part II: stability analysis, *Journal of Sound and Vibration* 178 (1994) 455–481.
[4] H.R. Oz, M. Pakdemirli, E. Ozkaya, Transition behavior from string to beam for an axially accelerating material, *Journal of Sound and Vibration* 215 (3) (1994) 517–578.
[5] M. Pakdemirli, A.G. Ulsoy, A. Ceranoglu, Transverse vibration of an axially accelerating string, *Journal of Sound and Vibration* 169 (1994) 179–196.
[6] M. Pakdemirli, E. Ozkaya, Approximate boundary layer solution of a moving beam problem, *Mathematics in Computer Applications* 2 (3) (1998) 93–100.
[7] F. Pellicano, F. Zirilli, Boundary layers and non-linear vibrations in an axially moving beam, *International Journal of Non-linear Mechanics* 33 (4) (1998) 691–711.
[8] R.G. Parker, Supercritical speed stability of the trivial equilibrium of an axially-moving string on an elastic foundation, *Journal of Sound and Vibration* 221 (2) (1999) 205–219.

[9] G. Chakraborty, A.K. Mallik, H. Hatwal, Non-linear vibration of a traveling beam, *International Journal of Non-linear Mechanics* 34 (1999) 655–670.
[10] H.R. Oz, M. Pakdemirli, Vibrations of an axially moving beam with time-dependent velocity, *Journal of Sound and Vibration* 27 (1999) 239–257.
[11] H.R. Oz, M. Pakdemirli, H. Boyaci, Non-linear vibrations and stability of an axially moving beam with time-dependent velocity, *International Journal of Non-linear Mechanics* 36 (2001) 107–115.
[12] L.Q. Chen, N.H. Zhang, J.W. Zu, Bifurcation and chaos of an axially moving viscoelastic string, *Mechanics Research Communications* 81 (2002) 81–90.
[13] C. Shin, J. Chung, W. Kim, Dynamic characteristics of the out-of-plane vibration for an axially moving membrane, *Journal of Sound and Vibration* 286 (2005) 1019–1031.
[14] N.H. Zhang, L.Q. Chen, Non-linear dynamical analysis of axially moving viscoelastic string, *Chaos, Solitons and Fractals* 24 (2005) 1065–1074.
[15] L.Q. Chen, W.J. Zhao, A conserved quantity and the stability of axially moving non-linear beams, *Journal of Sound and Vibration* 286 (2005) 663–668.
[16] L.Q. Chen, W.J. Zhabo, J.W. Zu, Simulation of transverse vibrations of an axially moving string: a modified difference approach, *Applied Mathematics and Computation* 166 (2005) 596–607.
[17] L.Q. Chen, X.D. Yang, Steady state response of axially moving viscoelastic beams with pulsating speed: comparison of two nonlinear models, *International Journal of Solids and Structures* 42 (2005) 37–50.
[18] A. Kartik, J.A. Wickert, Vibration and guiding of moving media with edge wave imperfections, *Journal of Sound and Vibration* 291 (2006) 419–436.
[19] L.Q. Chen, X.D. Yang, Nonlinear free transverse vibration of an axially moving beam: comparison of two models, *Journal of Sound and Vibration* 229 (2007) 348–354.
[20] K. Marynowski, T. Kapitaniak, Zener internal damping in modeling of axially moving viscoelastic beam with time-dependent tension, *International Journal of Non-linear Mechanics* 42 (2007) 118–131.
[21] J.L. Ha, J.R. Chang, R.F. Fung, Nonlinear dynamic behavior of a moving viscoelastic string undergoing three-dimensional vibration, *Chaos, Solitons and Fractals* 33 (2007) 1117–1134.
[22] M.H. Ghayesh, Non-linear vibration and stability comparison of two dynamic models of axially moving Timoshenko beams, *European Journal of Mechanics*, submitted for publication.
[23] M.H. Ghayesh, S.E. Khadem, Rotary inertia and temperature effects on non-linear vibration, steady-state response and stability of an axially moving beam with time-dependent velocity, *International Journal of Mechanical Sciences*, accepted for publication.
[24] J.J. Thomsen, *Vibrations and Stability*, Springer, Germany, 2003.
[25] A.H. Nayfeh, *Problems in Perturbation*, Wiley, New York, 1993.
[26] A.H. Nayfeh, D.T. Mook, *Nonlinear Oscillation*, Wiley, New York, 1979.
[27] A.H. Nayfeh, *Introduction to Perturbation Techniques*, Wiley, New York, 1981.